

# TUNE RESONANCE PHENOMENA IN THE SPS AND RELATED MACHINE PROTECTION

T. Baer\*, CERN, Geneva, Switzerland and University of Hamburg, Germany  
 B. Araujo Meleiro, T. Bogey, J. Wenninger, CERN, Geneva, Switzerland

## Abstract

The 7 km long CERN Super Proton Synchrotron (SPS) is, apart from the LHC, the accelerator with the largest stored beam energy worldwide of up to 3 MJ. In 2008, an equipment failure led to a fast tune shift towards an integer resonance and an uncontrolled loss of a high intensity beam, which resulted in major damage of the accelerator. Distinct experimental studies and simulations provide clear understanding of the beam dynamics and the beam loss patterns at different SPS tune resonances. Diverging closed orbit oscillations, a resonant dispersion and increased beta beating are the driving effects that lead to a complete beam loss in as little as 3 turns ( $69 \mu\text{s}$ ). At the moment, the commissioning of a new turn-by-turn position interlock system which will counteract the vulnerability of the SPS is ongoing.

In this paper, mainly the dynamics of beam losses at different tune resonances and machine protection related aspects are discussed. The beam dynamics at tune resonances are only briefly addressed, a more detailed description is given in [1]. A very comprehensive description of theory, methodology, experiments, simulations and results is given in [2].

## INTRODUCTION

On June 27<sup>th</sup>, 2008 an equipment failure in the SPS led to the uncontrolled loss of a high intensity beam at 400 GeV with a total beam energy of about 2.1 MJ. The vacuum chamber of a main bending magnet was punctured in the vertical plane (cf. Fig. 1) and the magnet had to be replaced. Cause of the incident was a freeze of the main timing system that inhibited the beam extraction after acceleration and resulted in an unintended tune shift towards the  $Q = 26$  integer tune resonance during the ramp down of the magnets. An analysis of the data from the beam loss monitoring system revealed that the beam was lost in less than 20 ms which is the time resolution of the system [3].

The incident points out a vulnerability of the SPS to fast beam losses and the challenge of machine protection against tune resonances.

## BEAM DYNAMICS AT TUNE RESONANCES

Dedicated experiments were made to understand the beam dynamics at different tune resonances in the SPS.

\* contact: Tobias.Baer@cern.ch

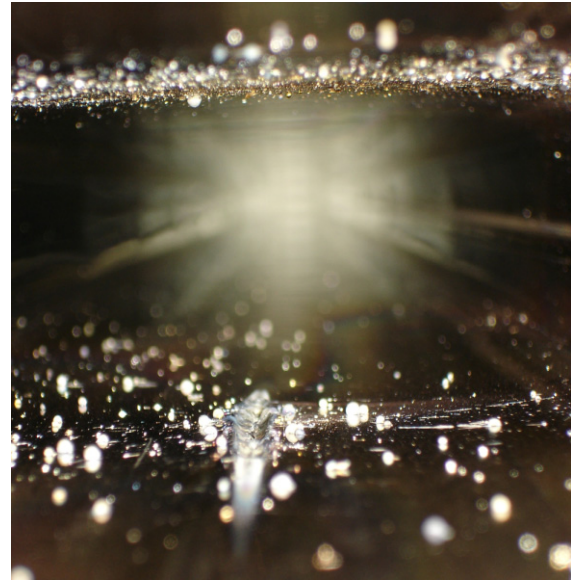


Figure 1: Impact of a 2.1 MJ beam. Over a length of about 10 cm the vacuum chamber is punctured. Metal droplets contaminate the vacuum chamber.

Figure 2 depicts the special threat of beam losses due to integer tune resonances.

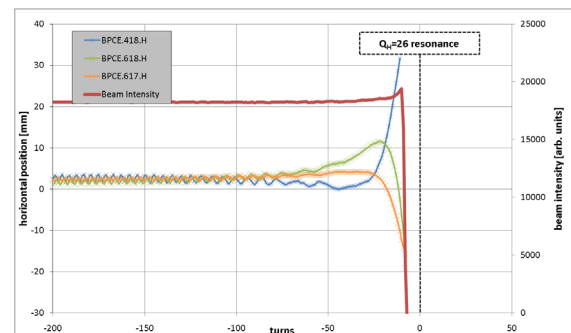


Figure 2: Beam intensity and horizontal turn-by-turn beam position at three particular beam position monitors (BPMs). The horizontal tune is decreased linearly by about  $-2 \cdot 10^{-3}/\text{turn}$ . The beam is lost at a tune of about  $Q_H = 26.015$ . **The complete beam is lost within 3 turns after the first beam losses start.**

Measurement conditions: beam energy: 450 GeV, bunch intensity:  $1.0 \cdot 10^{10}$  protons, 12 bunches.

The graph shows the horizontal beam position at three particular BPMs close to the  $Q_H = 26$  integer tune resonance and the corresponding beam intensity. The horizontal tune is decreased linearly and the beam position starts

to diverge about 40 turns before the resonance is reached, leading to a complete beam loss about 8 turns before the resonance peak would have been reached. Most challenging is the fact that it takes only 3 turns ( $= 69 \mu\text{s}$ ) to lose the complete beam after the first beam losses start. This leaves practically no reaction time for an adequate machine protection based on beam loss monitors (BLMs).

Besides these effects, tune resonances lead to a large variety of resonance phenomena. The effect on the closed orbit and the dispersion are described in the following sections. A detailed discussion is given in [1] and [2].

### Closed Orbit

Dipolar field errors lead to a distortion of the closed orbit which has a  $\frac{1}{\sin(\pi Q)}$  resonant behavior for integer tune values [2, p. 15]. The closed orbit resonance is the major cause of the diverging beam positions shown in Fig. 2<sup>1</sup>. Measurements and simulations<sup>2</sup> reveal that especially the nominal tunes of LHC-type beam ( $Q_H = 26.13$  and  $Q_V = 26.18$ )<sup>3</sup> are particularly close to the  $Q = 26$  integer tune resonance (cf. Fig. 3). An erroneous decrease of the tune will directly drive the closed orbit into resonance.

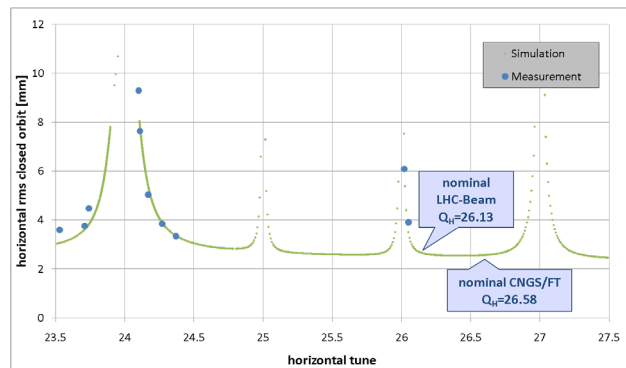


Figure 3: Simulation and measurement of the horizontal rms closed orbit as a function of the horizontal tune. The vertical tune is at nominal LHC-beam settings:  $Q_V = 26.18$ .

Measurement conditions: beam energy: 26 GeV, bunch intensity:  $4 \cdot 10^{10}$  protons, 12 bunches.

### Dispersion

Like the closed orbit, the dispersion has a  $\frac{1}{\sin(\pi Q)}$  resonant behavior for integer tunes [2, p. 15]. However, simulation and measurement<sup>4</sup> reveal an enormous  $Q_H = 24$

<sup>1</sup>Nevertheless, it needs to be pointed out that other resonance phenomena like diverging beta beating (cf. [2, p. 29]) increase the divergent behavior of the transverse beam position.

<sup>2</sup>cf. [2, p. 75] for details on the simulation.

<sup>3</sup>Since the horizontal working point is closer to the  $Q = 26$  integer tune resonance, the following discussion focuses on the horizontal plane only.

<sup>4</sup>The dispersion  $D = D_x$  is determined by measuring the beam position for different RF frequencies as described in [4, p. 152]. It is crucial to take into account that second order dispersion and momentum compaction

superperiodic<sup>5</sup> tune resonance (cf. Fig. 4). Due to the momentum-spread of about  $\frac{\Delta p}{p} = 1\%$  in the SPS, this enormous dispersion resonance leads to a diverging transverse beam size and related beam losses.

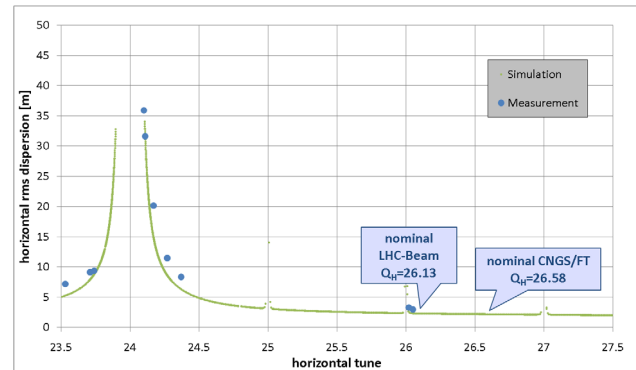


Figure 4: Simulation and measurement of the horizontal rms dispersion as a function of the horizontal tune.

Measurement conditions: beam energy: 26 GeV, bunch intensity:  $4 \cdot 10^{10}$  protons, 12 bunches.

Whereas the resonance condition for closed orbit distortion and dispersion are the same, the origins of both effects are different, what accounts for the different resonance behavior. The dispersion has its origin in *dipolar fields* that are dominated by the main bending fields that are distributed *periodically* around the accelerator. This leads to an extreme superperiodic dispersion resonance. In contrast, the closed orbit distortion is generated by dipolar field *errors* that are predominantly induced by quadrupole misalignments [5, p. 292]. These misalignments are to first approximation distributed *randomly*. As a result, the superperiodic  $Q_H = 24$  closed orbit resonance shown in Fig. 3 is far less pronounced than the superperiodic dispersion resonance. An analytical explanation is found in [2, p. 31 ff.].

## BEAM LOSS PATTERN

Experiments and MAD-X tracking studies have been done to understand the beam loss patterns of different equipment failure scenarios. A fast decrease of the quadrupole currents turned out to be especially threatening and is discussed in the following.

### Dynamics of Beam Losses

Because of the very different beam dynamics for different tune resonances, it is crucial to understand which tune resonances determine the beam losses. Under certain conditions, the crossing of an integer tune resonance is also

factor also have a diverging behavior for tune values around  $Q_H = 24$ . The latter results in a tune dependent relation between relative RF frequency trim and momentum offset.

<sup>5</sup>The SPS is constructed of six similar sextants, each consisting of 18 FODO cells.

possible. Figure 5 depicts a case where the  $Q_H = 26$  integer resonance is crossed without a measurable decrease of beam intensity. The beam is strongly excited by the resonance, which leads to large beam oscillations of up to 20 mm amplitude.

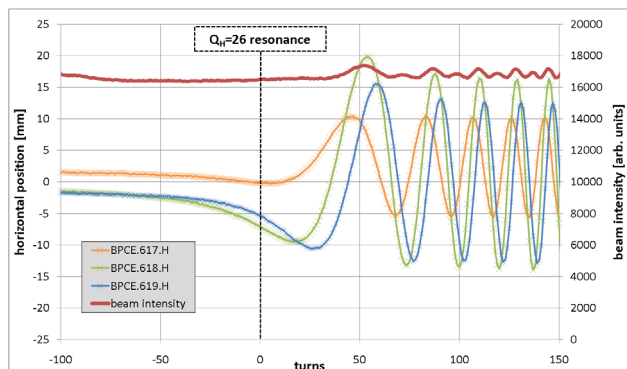


Figure 5: Horizontal turn-by-turn beam position at three particular BPMs and beam intensity. The horizontal tune is decreased linearly by about  $-4 \cdot 10^{-4}/\text{turn}$ . The beam crosses the  $Q_H = 26$  integer resonance without measurable losses but is strongly excited.

Measurement conditions: beam energy: 200 GeV, bunch intensity:  $1.0 \cdot 10^{10}$  protons, 12 bunches.

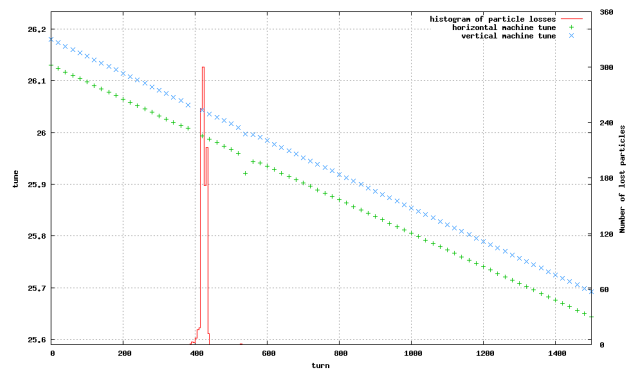
MAD-X tracking studies with a dynamic change of the quadrupole strengths were done. A detailed description of the tracking code is given [2, p. 34, 77].

Basically, three different types of loss patterns are observable for fast changes of the quadrupole strengths:

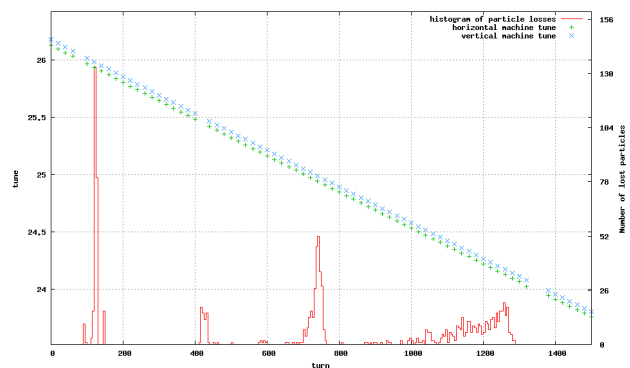
1. For tune changes of up to  $\approx 3 \cdot 10^{-4}$  per turn the beam is completely lost when reaching the  $Q_H = 26$  integer resonance (cf. Fig. 6a).
2. When the tune decreases faster than  $\approx 1.5 \cdot 10^{-3}$  per turn, the beam is able to partly cross the  $Q_{H/V} = 26$  integer resonance with significant beam losses at integer and half integer tune resonances (cf. Fig. 6b).
3. For even faster tune decreases the beam losses are determined by the  $Q = 24$  superperiodic tune resonance. Due to the extreme width of the superperiodic tune resonance the beam is lost well before the resonance maximum (cf. Fig. 6c).

The simulations are well consistent with experimental data [2, p. 34].

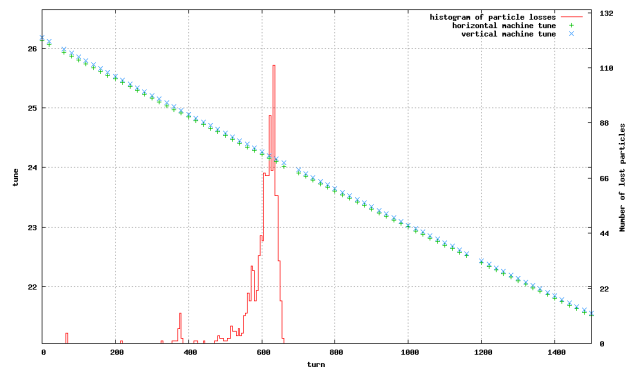
Fast failure tests of the main power converters showed that the slope of the tune is limited to about  $-3.4_{-0.3}^{+1.6} \cdot 10^{-3}$  [2, p. 46] at the  $Q = 26$  integer tune resonance due to the inductance of the circuits. This confirms that at least parts of the beam are able to cross the  $Q_{H/V} = 26$  integer tune resonance and are lost at lower tune resonances. In any case, the beam is strongly excited when crossing the integer resonance and significant orbit oscillations are observable.



(a) relative decay of quadrupole strengths of  $1 \cdot 10^{-5}$  per turn (tune slope  $\approx 3 \cdot 10^{-4}$  per turn).



(b) relative decay of quadrupole strengths of  $5 \cdot 10^{-5}$  per turn (tune slope  $\approx 1.5 \cdot 10^{-3}$  per turn).



(c) relative decay of quadrupole strengths of  $1 \cdot 10^{-4}$  per turn (tune slope  $\approx 3 \cdot 10^{-3}$  per turn).

Figure 6: Horizontal and vertical machine tune and a histogram of the particle losses. Depending on the slope of the tune, the integer tune resonances can be crossed. 1000 particles are tracked.

### Spatial Beam Loss Pattern

The SPS has a non-uniform aperture. Focusing quadrupoles are enlarged in the horizontal plane, defocusing quadrupoles in the vertical plane. There are also two groups of main bending magnets (MBA and MBB) with different apertures, depending on the local beta functions. The global aperture is limited by special elements like collimators or the internal beam dumps. Table 1 gives an

Table 1: Half-aperture of the main elements and special aperture-limiting elements in  $mm$  and multiples of the beam size  $\sigma$  for nominal LHC-beam ( $\epsilon_{H,V}^{n,1\sigma} = 3.5\mu m \cdot rad$ ) at injection energy (26 GeV).

	Element	Position	Half-Aperture HxV	
		[m]	[mm] × [mm]	[ $\sigma$ ] × [ $\sigma$ ]
<b>Main Elements</b>	MBA (close to QF)		71x17	21x8
	MBB (close to QD)		60x24	25x7
	QF		76x19	21x12
	QD <sup>6</sup>		42x42	26x12
<b>Special Elements</b>	TIDP (Scrapper)	456	41x15	<b>13x8</b>
	TIDH (Beam Dump)	573	55x27	16x16
	TIDV (Beam Dump)	603	43x20	24x6
	TCE (Collimator)	1692	65x24	37x7
	TPST (Collimator) <sup>7</sup>	1713	39x78	15x32
	TPSG (Collimator) <sup>7</sup>	4038	46x78	14x42
	TPSG (Collimator) <sup>7</sup>	6325	46x78	16x36

overview of the most important elements.

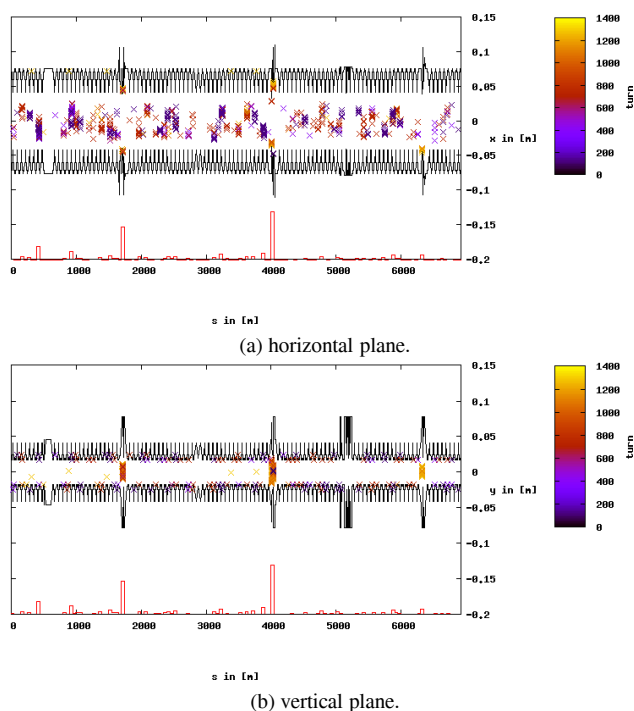


Figure 7: Spatial beam loss pattern of 1000 tracked particles. The crosses indicate the positions where the particles exceed the aperture (in black) for the first time. Crosses within the aperture limit are related to beam losses in the other plane. The color coding indicates the turn of the particle losses after the start of the simulation. A red histogram below the aperture indicates the amount of particles lost at the corresponding position.

The tracking conditions are the same as in Fig. 6b.

<sup>6</sup>The defocusing quadrupoles in the injection and extraction region have an increased half-aperture of 76 mm in the horizontal and 46 mm in the vertical plane.

<sup>7</sup>The TPST and TPSG collimators are fixed to the septum girders and can be retracted together with the septum magnets if no extraction is needed.

The MAD-X tracking studies on the dynamics of the beam losses also provide information on the spatial loss patterns. Figure 7 depicts a typical spatial beam loss pattern. Noteworthy is that the beam losses in the horizontal plane occur at very distinct aperture limiting elements. This is different for losses in the vertical plane: The B-type main dipoles have a very small aperture which is only  $1\sigma$  larger than the global aperture limit (cf. Table 1). Thus, increased beam losses occur at B-type main dipoles throughout the whole accelerator.

This shows that there is not always a clear beam loss hierarchy. The margin between aperture limit and protection devices is too small and not the whole phase space is covered, which underlines the need of an a priori protection against beam losses due to fast tune changes.

## MACHINE PROTECTION

The experiments and simulations as well as the 2008 incident underline the threat of fast beam losses due to tune resonances. Very localized beam losses in as little as 3 turns make the  $Q = 26$  integer tune resonance under nominal conditions the most critical one.

### Present Machine Protection Systems

The BLM system in the SPS has a time resolution of  $20\text{ ms} \hat{=} 870$  turns. It is by no means capable of protecting the SPS against fast beam losses in a few turns.

The SPS main quadrupole circuits are protected by an interlock on the quadrupole currents. Tests at 400 GeV revealed that the interlock system has a delay of 12 ms. In contrast, an experimental power cut of the main quadrupole circuits showed that under nominal LHC-beam conditions the  $Q_H = 26$  integer tune resonance would be reached in  $7.7^{+0.4}_{-0.5}$  ms [2, p. 43]. Thus, no protection against fast equipment failures is provided.



### New Fast Turn-by-turn Position Interlock

The experimental studies showed that in the vicinity of an integer tune resonance the beam position starts to oscillate typically 30 turns before beam losses are measurable. Based on this, the new fast beam position interlock system will counteract the vulnerability of the SPS (cf. Fig. 8).

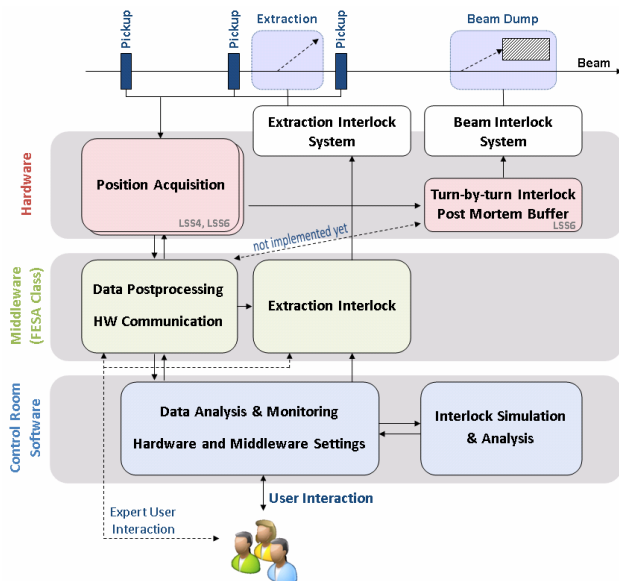


Figure 8: Layout of the new position acquisition and position interlock system. The turn-by-turn position interlock is processed in the hardware, the extraction interlock by the middleware software. The control room software provides the user interface including an analysis module. A detailed description of the new interlock system is given in [2, p. 51 ff.].

For the position acquisition six stripline coupler BPMs in two groups with a betatron phase advance of about  $45^\circ$  between two BPMs are used (only three BPMs are used for the turn-by-turn position interlock). The acquisition hardware is based on logarithmic amplifiers that provide a large dynamic range. Each turn ( $23 \mu\text{s}$ ) an FPGA does the interlock processing and sends a beam dump signal to the beam interlock system in case the current beam position is out of a dynamic reference window around the average position. The total reaction time is about one turn.

Based on the experimental data, a novel dynamic interlock algorithm was developed that showed perfect performance in offline-tests [2, p. 59].

For post analysis, it is planned that a post mortem buffer stores the data of all three BPMs of the last 1000 turns. The buffer is frozen when a beam dump request is sent by the system. The data is automatically transferred and stored in the logging data base.

The system also provides a new robust extraction interlock to LHC and CNGS target on the beam position. For each BPM, it compares the average position of about 50 turns to a reference window. The interlock processing is done by the middleware.

The whole system is currently in the commissioning phase.

### ACKNOWLEDGMENTS

The contribution of many colleagues is gratefully acknowledged. In particular the author would like to thank E. Elsen, K. Fuchsberger, L. Jensen, R. Jones, J. Savioz and R. Steinhagen for fruitful discussions and their contributions to the interlock system.

### REFERENCES

- [1] T. Baer, B. Araujo Meleiro, T. Bogey and J. Wenninger, "Tune Resonance Phenomena in the SPS and Machine Protection via Fast Position Interlocking", IPAC'10, Kyoto, 2010, TUPEB036, p. 1602.
- [2] T. Baer, J. Wenninger and E. Elsen, "Tune Resonance Phenomena in the SPS and related Machine Protection", CERN-THESIS-2010-097, Geneva, 2010.
- [3] J. Wenninger, "SPS Machine Protection Incident in 2008", CERN-BE-Note, Geneva, 2009.
- [4] M. G. Minty and F. Zimmermann, "Measurement and Control of Charged Particle Beams", Springer-Verlag, Heidelberg, 2003.
- [5] F. Hinterberger, "Physik der Teilchenbeschleuniger und Ionenoptik", Springer-Verlag, Heidelberg, 2008.